IOPscience iopscience.iop.org

Home Search Collections Journals About Contact us My IOPscience

Dynamic observations of nanoscale self-assembly on solid surfaces

This article has been downloaded from IOPscience. Please scroll down to see the full text article.

2002 J. Phys.: Condens. Matter 14 4227

(http://iopscience.iop.org/0953-8984/14/16/313)

View the table of contents for this issue, or go to the journal homepage for more

Download details:
IP Address: 171.66.16.104
The article was downloaded on 18/05/2010 at 06:31

Please note that terms and conditions apply.

INSTITUTE OF PHYSICS PUBLISHING JOURNAL OF PHYSICS: CONDENSED MATTER

J. Phys.: Condens. Matter **14** (2002) 4227–4240 PII: S0953-8984(02)30347-3

Dynamic observations of nanoscale self-assembly on solid surfaces

R Plass[1], **N C Bartelt**[2] **and G L Kellogg**[1]

[1] Sandia National Laboratories, Albuquerque, NM 87185-1415, USA
[2] Sandia National Laboratories, Livermore, CA 94551-0969, USA

Received 31 October 2001, in final form 29 January 2002
Published 11 April 2002
Online at stacks.iop.org/JPhysCM/14/4227

Abstract

Using low-energy electron microscopy, we find that Cu and Pb, arranged in single atomic layers on the Cu(111) surface, self-assemble into ordered, nanoscale domain patterns. The pattern type, feature size, and degree of long-range order vary controllably with surface composition and temperature. The continuous evolution of the domain structures from circular islands to stripes to 'inverted' islands with increasing Pb coverage agrees with theoretical predictions and simulations based on the existence of competing long- and short-range interactions. The details of the self-assembly process depend on a number of factors including temperature, surface morphology, and the presence of small amounts of sulfur.

1. Introduction

There is considerable current interest in devising means to fabricate structures on surfaces at the nanometre scale. Although a great deal of work has focused on engineering nanostructures by direct manipulation, such processes are too slow for most applications. An attractive, alternative approach is to form patterns of nanometre dimensions on solid surfaces and then grow the nanostructures on these templates. In this case, large numbers of identical nanostructures can be formed simultaneously. To follow this approach and create patterns in a controllable manner with the proper dimensions, one needs an understanding of the thermodynamic and kinetic processes governing the self-assembly.

The formation of nano-templates on surfaces is complicated by the fact that for two-dimensional, two-phase systems with only short-ranged attractions between atoms, small domains are not thermodynamically stable, i.e., small domains coarsen into large domains with time. This is true whether the two phases are islands of one material on top of the other or two different structures of the same surface. It costs energy to make a step or a domain boundary between phases, so the surface minimizes this energy by reducing the step or boundary length. If, however, in addition to the short-range attractive interactions, there are longer-range repulsive interactions, the competition between the repulsive interaction,

 © 2002 IOP Publishing Ltd Printed in the UK

which favours small domains, and the energy required to make domain boundaries can lead to domain stabilization and two-dimensional self-assembly [1–10]. The characteristic feature length of the pattern depends on the ratio of the boundary formation energy to the long-range interaction energy and can be of nanometre-scale dimensions. This type of domain stabilization has been observed in widely varying chemical and physical systems including magnetic thin-film structures [1–6] and molecular compounds at the air–water interface [7–10]. In these examples repulsive interactions are due to magnetic and electric dipole interactions, respectively. Beautifully ordered patterns of circular domains (droplets) and stripes, which can be manipulated by applied magnetic or electric fields, are observed in these systems.

It has been shown that elastic interactions resulting from surface stress differences between different atomic structures will give rise to such domain stabilization on solid surfaces [11,12]. One can qualitatively understand how stress differences can lead to domain stabilization by considering the situation where one surface phase is under compressive and the other under tensile stress. At each domain boundary there will be elastic relaxations because the compressive surface phase can expand into the tensile phase. This relaxation will lower the surface energy and favour the creation of domain boundaries, i.e. favour the formation of many small domains. Furthermore, the stabilization associated with elastic relaxations of each boundary increases with decreasing boundary separation. However, as mentioned earlier, small domains increase the total domain boundary length and increase the energy of the system. This competition leads to the formation of thermodynamically stable domains with a characteristic size l_0 determined by the ratio of the boundary and surface stress differences. If the boundary between phases is sharp, then

$$l_0 = \pi a \exp(C_1/C_2 + 1) \tag{1}$$

where C_1 is the boundary energy per unit length, C_2 is proportional to the square of the difference in stress between phases, and a is a length which measures the sharpness of the interface between boundaries.

Analytical models and simulation studies [13–18] based on this type of competition predict interesting thermodynamic behaviour for such systems. One of the most intriguing predictions is about how the domain pattern changes with increasing area fraction of one phase with respect to the other. According to the models, the pattern should evolve from circular islands of one phase within the matrix of the other (called the droplet phase) to alternating rows of the two phases (called the stripe phase) to circular islands with the phases reversed (called the inverted droplet phase) [9, 13, 16–18]. Despite the fundamental nature of this prediction and despite the many observations of self-assembled structures on surfaces that have been attributed to stress interactions [19–24], the predicted pattern evolution with changing area fraction was not observed until our recent report of self-assembly of Pb structures on Cu(111) [25].

In this paper we review the experiments leading to this discovery. The details of the dynamic processes involved in self-assembly are described, as are the effects of Pb coverage and sample temperature. We also make some qualitative observations about the kinetic behaviour of observed structures and speculate about the properties that are required for a thin-film solid system to exhibit two-dimensional self-assembly.

2. Experimental details

Our direct observations of domain evolution during self-assembly are made possible by the unique attributes of the low-energy electron microscope (LEEM) [26]. Conceptually, the LEEM is an electron-optical analogue of an ordinary light microscope: instead of light and optical lenses, electrons and magnetic or electrostatic lenses are used, leading to significantly

enhanced spatial resolution. In our instrument the spatial resolution is 7–8 nm. The use of electrons also provides a variety of imaging modes and contrast mechanisms, the details of which can be found in papers by Bauer [26] and Tromp and Reuter [27]. Moreover, because it is a non-scanning microscope, the LEEM allows one to view dynamic processes on surfaces in real space and with a time resolution limited by the image recording device. In this study we use a commercial LEEM after Bauer's design [26], which has been modified to include ultrahigh-vacuum chambers for Auger electron spectroscopy and Ne-ion sputtering.

The details of the experimental set-up and the procedures used to prepare clean Cu surfaces have been described in earlier articles [28]. In this study Pb was deposited on the Cu(111) surface at rates between 0.02 and 0.04 ML min^{-1} from a heated PBN crucible holding 99.999% pure Pb. No energetic Pb ions impact on the sample with this set-up. The temperature of the Pb in the crucible was not measured, but it was well above the Pb melting point (600 K). The line-of-sight from the doser to the sample was 80° off normal, which can lead to non-uniform deposition across the sample. However, we did not notice any non-uniform deposition over our small fields of view (typically a few microns). The sample temperature was typically held above the Pb melting point during deposition, resulting in slow desorption of Pb when the flux was turned off. For these reasons coverage determinations were made by direct observations of the LEEM images and not from the flux of Pb atoms. The background pressure in the system was typically in the low- to mid-10^{-10} Torr range during Pb deposition. We used dark-field imaging on the (4×4) diffraction spots identify regions of the incommensurate phase. These images were not very intense so, to follow the domain evolution, we used bright-field imaging (images formed from the (0, 0) LEED beam) at an electron energy where the incommensurate phase appeared bright.

3. The Pb/Cu system

The two surface phases of Pb on Cu that exhibit self-assembled domain structures are: (1) a disordered Pb/Cu surface alloy phase and (2) an incommensurate Pb overlayer phase. The surface alloy phase is obtained by vapour deposition of Pb on the clean Cu(111) surface at room temperature and above. The overlayer phase forms after completion of the surface alloy phase at 0.22 ML and completely covers the surface at 0.56 ML. Here, one monolayer is defined as one Pb atom per surface Cu atom. The atomic structures of these two phases and their thermodynamic properties have been well characterized by low-energy electron diffraction (LEED) [29–31], spot-profile-analysis LEED (SPA-LEED) [32, 33], STM [30, 34], helium-atom scattering [35], and surface x-ray diffraction [36]. These studies show that the surface alloy phase consists of Pb substituted into the top Cu(111) surface layer. Local regions of $p(2 \times 2)$ and $(\sqrt{3} \times \sqrt{3})R30^\circ$ appear in STM images [34], but long-range order does not exist. The Pb overlayer structure has a lattice constant close to $4/3$ that of the Cu substrate, but the lattice constant varies significantly with Pb coverage and sample temperature. The LEED pattern from the overlayer phase exhibits reasonably sharp diffraction spots near the (4×4) locations [29–33].

4. Results and discussion

4.1. Constant-temperature measurements

A series of LEEM bright-field images illustrating the initial growth of the Pb overlayer phase on the Pb/Cu surface alloy phase at a temperature of 673 K are shown in figure 1. In these and subsequent images the electron energy is 18–20 V. At this energy, the overlayer phase is

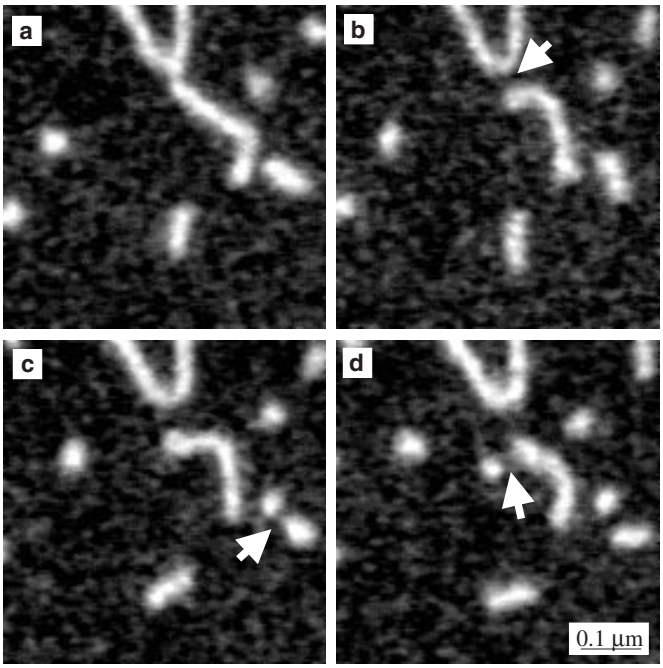

Figure 1. LEEM images of domain nucleation events during Pb deposition on Cu(111) at 673 K. The Pb overlayer phase is bright and the surface alloy phase is dark. (*a*) An overlayer-phase stripe is expelled from a stripe pinned to a step. (*b*) The expelled stripe is pinched off. (*c*), (*d*) Pinched-off stripes break up into two-dimensional islands (droplets). The time interval between frames is roughly 0.35 s.

bright and the surface alloy phase is dark. The overlayer phase first appears at steps and grows into stripes pinned at the lower edge of the steps. The hairpin-like feature at the top of figure 1 is a stripe of the overlayer phase pinned to a step in the Pb/Cu alloy surface. Note that a few islands of the overlayer phase also nucleate on the flat terrace. As more Pb is deposited, the width of the stripe increases to a fixed size (several tens of nanometres) and stops growing. Additional Pb in the overlayer phase is expelled from the stripe in a snake-like fashion and breaks off from the pinned stripes (see the arrow in figure 1(*b*)). As the expelled stripes move out onto the terrace, they break into circular islands or 'droplets' (figures 1(*c*) and (*d*)). The pinched-off droplets move on to the terrace and along with the self-nucleated droplets form a fairly disordered pattern (ordering of the droplet patterns is discussed later).

When the density of droplets is low, the droplets move in a random, Brownian-like manner. As more Pb is deposited, the density of droplets increases and repulsive interactions between the droplets become apparent. At sufficiently high densities, the droplet motion is severely constrained (figure 2(*a*)), and the droplets begin to form ordered patterns. (The images in figure 2 are from the same region of the surface as figure 1.) It is important to note that the droplets are incorporated into the ordered pattern far from the places where they were created—the droplets can move more than a micron before being incorporated into the more ordered structure. The droplets shown in figure 2(*a*) have a size distribution peaking at 67 ± 8 nm, with significant temporal fluctuations in area and shape. Additional Pb deposition leads to an interesting phenomenon. The droplets coalesce and form stripes on the terraces (figure 2(*b*)). Like the droplets, the domain walls of the stripes also exhibit correlated oscillations. The width

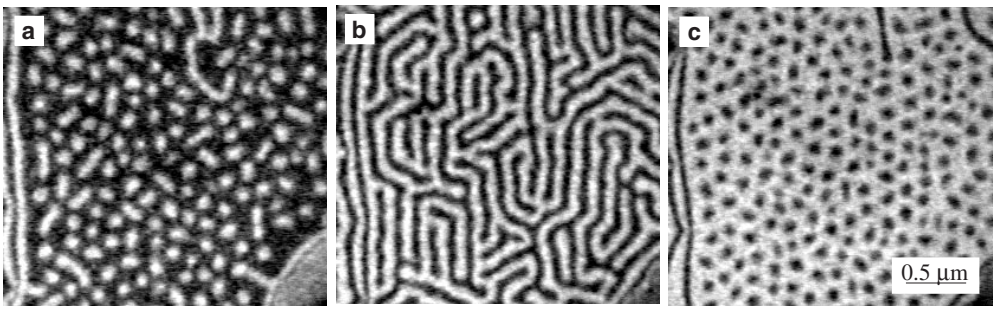

Figure 2. LEEM images of domain pattern evolution as a function of Pb coverage at 673 K subsequent to the nucleation events shown in figure 1. The images correspond to Pb coverages of (*a*) 0.33, (*b*) 0.39, and (*c*) 0.48 ML. The time interval between images is roughly 400 s. The evolution from droplets to stripes to inverted droplets is evident (images from [25]).

of the overlayer-phase stripes increases, to a limited extent, with increasing Pb deposition. There is a concomitant reduction of the width of the surface alloy stripes (black) until domain wall fluctuations pinch off circular islands of the surface alloy phase in the matrix of the overlayer phase (figure 2(*c*)). The correlated motion of these inverted droplets is the same as the original droplets in figure 2(*a*). As the Pb monolayer is completed, the inverted droplets disappear and the surface is covered entirely by the overlayer phase. As we reported earlier [25], the progression from droplets to stripes to inverted droplets with increasing area fraction of the overlayer phase is a signature of two-dimensional, two-phase systems with competing short-range attractive and long-range dipolar repulsive interactions [9, 13, 16–18]. We propose that the repulsive interaction arises from a stress difference between the two phases [25].

A surprising feature of this system is that when the Pb deposition is carried out at temperatures only 22 K colder than the sequence reported above, the nature of the nucleation mechanism changes significantly. As the overlayer phase is expelled from the pinned regions at the lower side of the steps, the snake-like stripes move out on to the terrace as above, but instead of breaking into droplets, they remain intact. An example of stripe nucleation without droplet formation is shown in figure 3. In this sequence Pb deposition is carried out at 651 K. The subsequent images in figure 4 show that the stripe phase remains throughout the entire coverage regime, i.e., neither droplets nor inverted droplets are formed. We have confirmed the metastability of the stripes by increasing the temperature while holding the coverage fixed at a value where we would expect droplets to form. Under these conditions, the stripes irreversibly break into droplets by domain boundary oscillation 'pinch-off' events. The conclusion from these measurements is that, at these lower temperatures, domain wall fluctuations are insufficient to allow for the pinch-off events that lead to droplet formation. This metastability is consistent with theoretical models of the stripe energetics [16]. The fundamental difference in pattern evolution corresponding to a temperature difference of only 22 K provides a vivid illustration of the importance of both thermodynamics and kinetics in two-dimensional self-assembly.

4.2. Constant-coverage measurements

The above measurements show how it is possible to achieve a variety of pattern types by changing the coverage of the overlayer phase at a fixed temperature. We have found that the complementary procedure of changing the temperature at fixed coverage can be used to control the characteristic feature size. Figure 5 shows LEEM images illustrating the pattern evolution

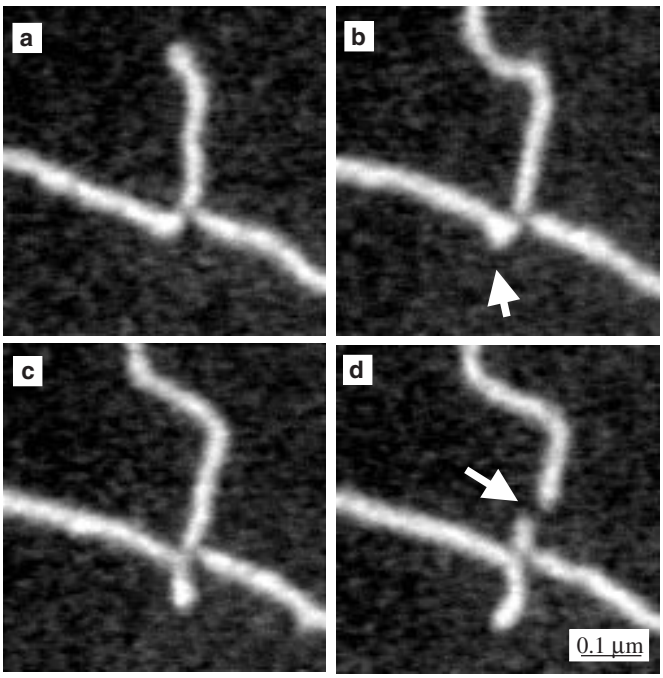

Figure 3. LEEM images of domain nucleation events during Pb deposition on Cu(111) at 651 K. Metastable stripes nucleate and grow with very few pinch-off events occurring—one of which is shown in image (*d*). The time interval between frames is 0.9 s.

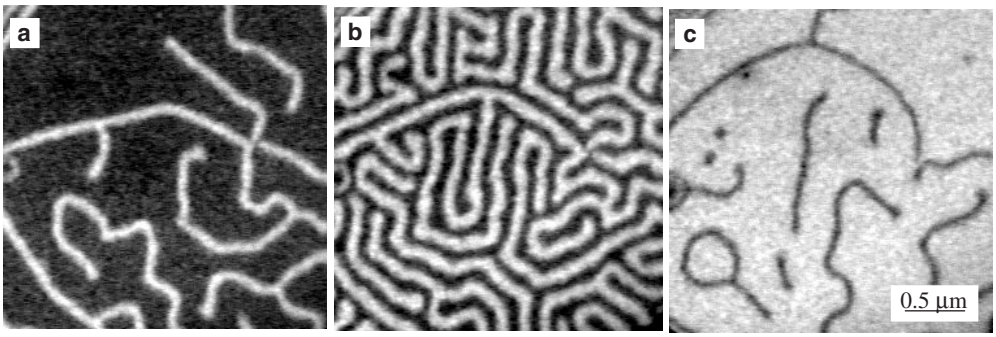

Figure 4. LEEM images of domain pattern evolution as a function of Pb coverage at 651 K subsequent to the nucleation events shown in figure 3. The images correspond to Pb coverages of (*a*) 0.26, (*b*) 0.39, and (*c*) 0.51 ML. The droplet and inverted droplet phases do not appear. The low- and high-coverage stripes are metastable as discussed in the text.

at fixed coverage with changing temperature. Images (*a*)–(*c*) show the temperature dependence of inverted droplet size and images (*d*)–(*f*) show the temperature dependence of stripe width. In both cases the feature size clearly diminishes as the temperature is increased. This observation, which is predicted by theory [13,15,37], suggests a means to control the feature dimensions of a given domain pattern. The inverted droplet images shown in figures 5(*a*)–(*c*) also illustrate the degree of order that can be achieved in this system [25]. The structures are clearly hexagonal,

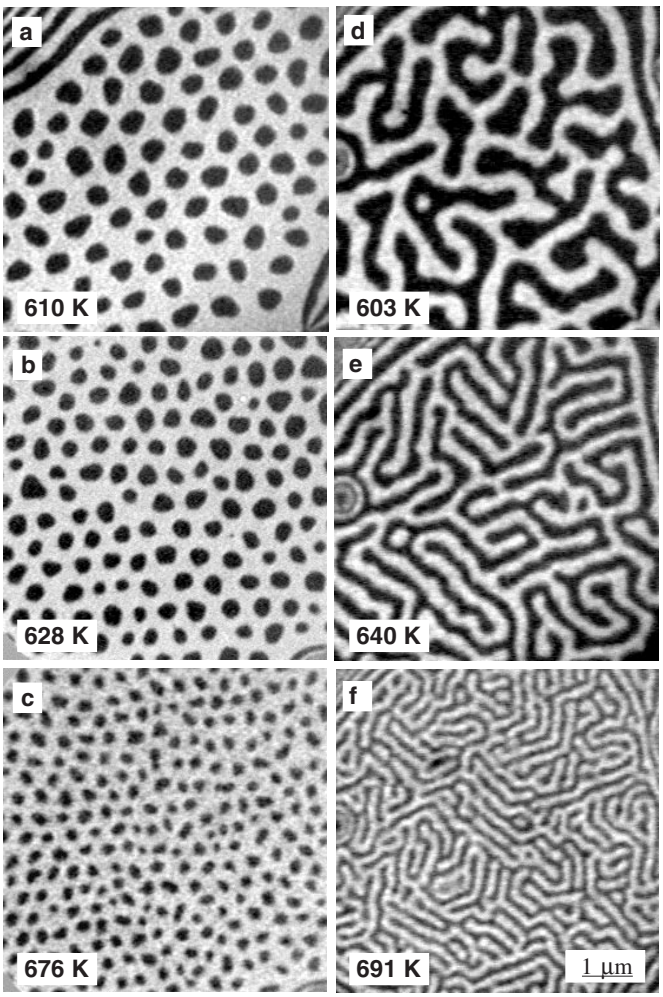

Figure 5. LEEM images showing the temperature dependence of the characteristic feature size for inverted droplets ((*a*)–(*c*)) and stripes ((*d*)–(*f*)). The droplet diameters and stripe widths decrease with increasing temperature. The long-range order in the inverted droplet phase disappears at higher temperatures.

i.e., the droplets form a close-packed array. As the temperature is increased, a transition from an ordered to a disordered structure is observed. The kinetics of the stripe pattern evolution shown in figures 5(*d*)–(*f*), are very intriguing, resembling 'fingering' instabilities observed in magnetic fluids [5].

To qualitatively explain the variation of feature size, we point out that according to equation (1), the log of the characteristic feature length is given by the ratio of the domain boundary energy to the square of the surface stress mismatch. For comparison to these models, we show a semi-log plot of stripe width versus temperature in figure 6. The linear decrease is consistent with the linear decrease expected [38] for boundary energy near an Ising-like critical point. We thus attribute the variation in feature size to the decrease in boundary free energy due to increased thermal boundary fluctuations as the temperature is increased.

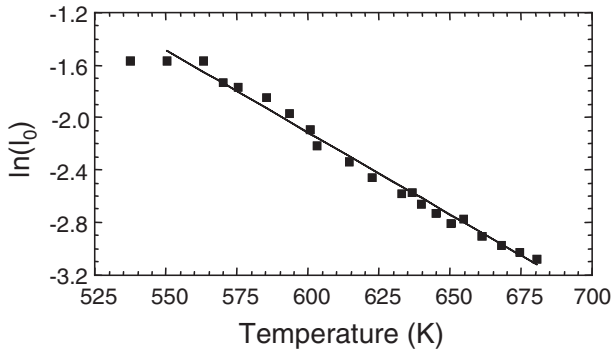

Figure 6. A semi-log plot of the average stripe width versus temperature for an area fraction of 0.5. The implications of the roughly linear relationship are discussed in the text.

4.3. Mass transport during overlayer growth

As described in section 4.1, self-assembly in this system readily occurs because of the large mobility of individual domains containing tens to hundreds of thousands of atoms. Droplets formed at pinned steps (shown in figure 1) move distances of more than a micron on a timescale of tens of seconds before becoming compacted into dense patterns (figure 2(*a*)). The atomic processes governing this mobility are not at present known. In the similar Sn-on-Cu(111) system, comparably sized islands of the overlayer phase were also observed to have a remarkably large mobility [39]. By examining the speed of the islands as a function of island radius, it was shown in this case that the large mobility was a result of rapid diffusion of Sn from one side of the island to the other side, through the interior of the island. Another possible scenario is that rapid diffusion along the edge of the overlayer phase determines the mobility, as is observed for much smaller islands on other metal surfaces (see, e.g. [40]). However, in this case the mobility decays as the inverse cube of the droplet radii and it is not clear that edge diffusion can account for the mobility of the large size range of droplets that we observe. Edge diffusion would also not account for our observation of the large fluctuations in island area. For such large-scale motion, Pb–Cu exchange at the island edge must be facile. Centre-of-mass motion could then result from small biases in a large, random, thermal Pb–Cu exchange rate on one side of the island compared to the other. Detailed analysis of the island motion is in progress to resolve this issue.

Important insight into the atomistic processes taking place during the growth of the overlayer and the movement of droplets is obtained by observing the behaviour of vacancy islands as the Pb overlayer grows on the surface alloy. Figure 7 shows LEEM images recorded during such a growth sequence. The features indicated by the arrows are a vacancy island and a step edge. The identification of a vacancy island (as opposed to an adatom island) is based on the observation that the overlayer phase grows inwards from the island edge. As noted above, the overlayer phase always grows out from the step bottoms. As the overlayer phase increases in coverage, the vacancy island increases in size (figures 7(*b*)–(*d*)), indicating that Cu atoms are consumed during the growth of the overlayer phase. It is known from the STM work of Nagl *et al* [34] that the Cu layer that resides directly under the Pb overlayer phase is pure Cu. To form the overlayer phase, Cu atoms are required to fill in the vacancies left by the transport of Pb atoms from the surface alloy phase to the overlayer phase. It is interesting to note that this is just the opposite of what is observed for Pb on Cu(100), where LEEM observations [28] show that adatom islands grow during the transition from the c(4×4) surface alloy phase to

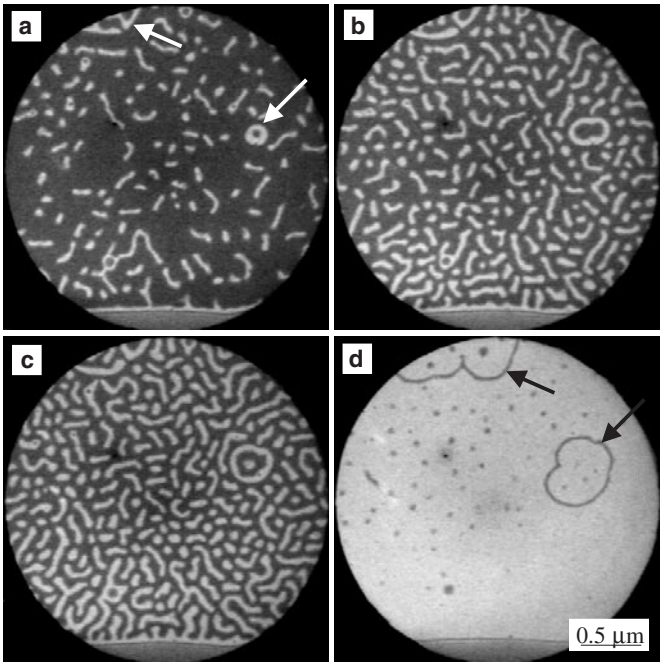

Figure 7. LEEM images of Pb deposition onto the Pb/Cu(111) surface alloy phase at 670 K showing the growth of a vacancy island (downward-pointing arrow) and the movement of a step (upward-pointing arrow). The behaviour of both is consistent with the removal of 0.09 ML of copper from the step edges to replace the surface vacancies left behind as the Pb is incorporated into the overlayer phase.

the c(2 × 2) overlayer phase (i.e., Cu atoms are expelled from the terraces and attach to the step edges).

4.4. The relationship between the configuration of surface steps and domain patterns

As already mentioned, the Pb overlayer phase first appears by decorating step edges. Because of the large thermal fluctuations in this system, we attribute this effect to an energetic preference for domain boundaries to occur at step edges (as opposed to a kinetic effect). (A similar interaction of domain boundaries with steps edges has been observed on Si(111) [41].) Despite this attractive interaction, notice that the width of the stripe decorating the step edges is very close to the width of the stripes formed on the terraces (see, for example, figure 2). This is consistent with theory: as the stripe grows away from the step edge, the elastic relaxations lower the energy of each domain boundary. When this decrease becomes large enough to overcome the cost of increasing boundary length, stripes form on the terraces. This critical stripe width depends on the cost of boundaries on the terrace, rather than the energy of the boundary near the step edge, and hence the stripe decorating the step edge has the same width as those on the terraces.

We also observe indications of a strong influence of domain boundary configurations on step structure. The Cu sample cleaning procedure produces a (111) surface that contains many step bunches. The steps in the bunches are typically curved due to the way in which they are formed: during the annealing periods, steps continuously flow past pinning sites, bend and form into bunches. Figure 8 shows a region of the Cu surface with numerous pinning sites

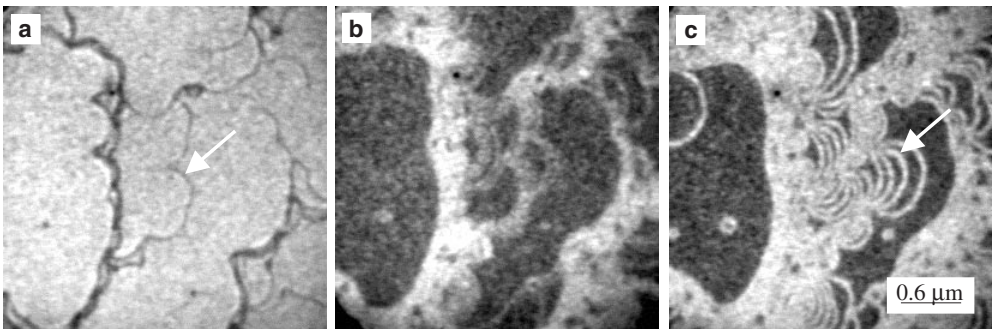

Figure 8. LEEM images of Pb deposition onto the Cu(111) surface, showing the effect of the overlayer phase on the terrace widths between steps in step bunches. (*a*) Bare Cu(111) surface. (*b*), (*c*) After enough Pb deposition to produce the overlayer phase. The step-to-step spacing in the region indicated by the arrow increases steadily with increasing overlayer coverage up to the half area fraction.

and the step bunches that they produced. We showed above that in the case of the flat regions of the surface, the first overlayer regions appear as underside decorations of surface steps. As Pb deposition proceeds, the width of this decorated region increases. In the case of a step bunch, decorations also appear as underside decorations. However, we find that the step-to-step spacing also increases substantially and steadily with increasing overlayer coverage. In regions between step pinning sites the step bunch regions expand at the expense of the flat terraces. Figure 8 shows how the width of the expansion depends strongly on the area fraction. As the area fraction of the overlayer phase increases, so does the distance between steps in the step bunches. The white arrow points to a region on the surface where the terrace width between steps in a bunch has expanded. Both the surface alloy alone and the overlayer alone covering the surface have step-to-step spacing in the step bunches essentially equal to the spacing for bare copper. But the Pb coverage corresponding to an area fraction of one half, where the surface alloy and overlayer phases have equal widths, yields step-to-step spacing thirty times larger (on average) than for the clean copper for step bunches with well separated pinning sites and flat terraces on either side. Beyond the half area fraction, the width of the overlayer decoration increases at the expense of the surface alloy, but the total width of the step bunch falls. Figure 9 shows a sequence of LEEM images indicating the retraction of a step bunch as the overlayer phase is completed.

To qualitatively explain this effect, we note that the spacing of steps in a step bunch around a pinning defect depends on the details of a balance between the interaction between steps and the stiffness of steps against bending [42]. A larger step–step repulsion produces a larger separation. For steps surrounded by a single phase, step–step interactions are relatively weak and fall off like the inverse square of the step separation with an elastic dipole strength proportional to the surface stress multiplied by the atomic step height [43]. The interaction between stripes has the same inverse square dependence [44], but with a dipole strength proportional to the stress difference between the phases composing the stripe multiplied by the stripe width. Since the stripe width is orders of magnitude larger than the step height, the elastic repulsions between stripes can be expected to dominate the normal step–step interaction. So we attribute the spreading of the step bunch to this large elastic interaction between the stripes decorating the step edges. (This is consistent with the observation of an increasing separation with increasing width of the stripe decorating the step.)

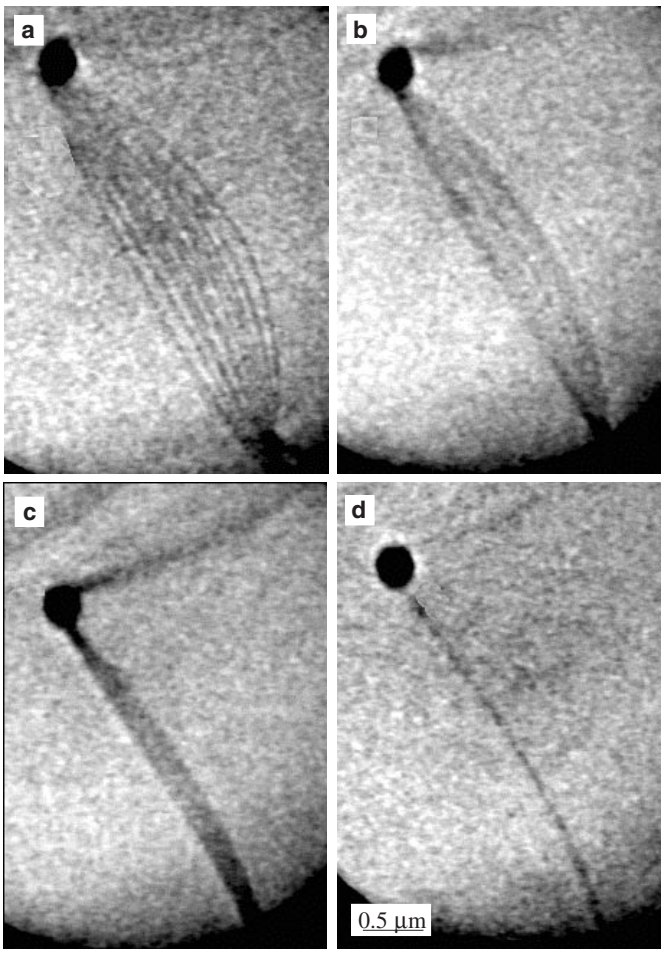

Figure 9. LEEM images of Pb deposition onto an Pb overlayer surface (area fraction ∼0.9) at 613 K illustrating the collapse of a pinned step bunch with increasing Pb.

This relationship between domain structure and surface morphology is related to that observed for Si surfaces [45,46] and could be expected to occur on the basis of thermodynamic arguments [47]. However, it requires a considerable amount of surface diffusion to occur and is a noteworthy consequence of the large atomic mobilities associated with this system.

4.5. Sulfur effects

Sulfur is a common contaminant in copper single crystals. To prevent sulfur from segregating to the surface during the experiments and during sample cleaning at elevated temperatures, considerable effort is devoted to removing sulfur from the near-surface region of the sample. Most of the near-surface sulfur is removed by heating the crystal to 1073 K in a flowing argon–hydrogen mixture prior to its introduction in the vacuum chamber. After placing the sample in the vacuum chamber, several cycles of ion sputtering and annealing are then carried out to reduce the level of sulfur to below the detection limit of Auger electron spectroscopy. Nevertheless, it is still possible that very low levels of sulfur are present on the (111) surface

during the experiments. It is therefore important to assess the effect of sulfur on the Pb–Cu self-assembly process.

To bring sulfur to the surface intentionally, we carried out high-temperature (1175–1275 K) anneals on samples that had not been treated with the *ex situ* furnace anneal. The sulfur concentration was monitored with a cylindrical mirror analyser Auger electron spectrometer using the positive portion of the differentiated S LMM Auger peak between 143 and 147 eV. The highest sulfur coverage that we investigated came from a surface that displayed a sulfur-induced $\left|\begin{smallmatrix} 4 & 1 \\ -1 & 4 \end{smallmatrix}\right|$ (matrix notation) reconstruction on about 75% of the surface. The known sulfur coverage of this phase, 0.35 ML [48], was used to calibrate the Auger signals of the other data in terms of sulfur monolayers.

The presence of S has relatively minor effects on the equilibrium structure of the domain patterns—even at the highest coverages, the characteristic size changes only by a small amount. Given the exponential dependence of the characteristic size on the boundary energy (equation (1)), this suggests that the changes in boundary energy due to small amounts of S are relatively small.

However, S has a striking influence on the kinetics of the self-assembly. The droplet motion is faster, and S changes the temperature required to break up metastable stripes and form droplets. Recall from the discussion above that it is possible to form stripes in the coverage regime where droplets are thermodynamically stable by carrying out the deposition at lower temperatures. When the temperature at this fixed coverage is increased, the metastable stripes break up into droplets. For systems in which the Cu is thoroughly cleaned by numerous sputter/anneal cycles, the metastable transition temperature is 700 K. However, when very small coverages of sulfur (0.05 ML) are present, the metastable transition temperature falls to less than 610 K. Using the number of cleaning cycles as a qualitative measure of sulfur, it appears that the metastable transition temperature decreases monotonically with coverage between 0 and 0.05 ML of sulfur (below 0.05 ML the Auger signal is in the noise). The lowering of the temperature required to transform stripes into droplets suggests that the presence of sulfur increases the speed of the domain boundary oscillations. With larger amounts of sulfur (from 0.10 to 0.25 ML), there is a gradual rise in the metastable transition temperature to approximately 660 K. The origin of this effect is not yet understood. However, we note that S is known to dramatically increase Cu self-diffusion on Cu(111) surfaces [49, 50], suggesting that the mobility of droplets and boundary fluctuations are limited by Cu (rather than just Pb) diffusion. Although more work is needed to fully understand the effect of sulfur on the self-assembly, it is important to realize that very small amounts of sulfur, even below the detection limit of Auger electron spectroscopy, can have a significant effect on the self-assembly process.

5. Summary

The real-time observations of the formation of domain patterns of lead on copper that LEEM provides gives some important new insights into the atomic processes which need to be manipulated in order that self-assembly can be controlled:

(1) Each domain is often nucleated far from the place where it is incorporated into the final domain pattern. Thus, in this system, self-assembly into ordered, large-scale domain patterns only occurs because of the large mobility of individual domains. Given this crucial importance of domain mobility, much more work needs to be done to understand the atomic mechanisms behind it. For the purposes of creating domain patterns, it is encouraging that the mobility can be enhanced by impurities, such as S.

(2) The stripe phase can readily be created as a metastable phase (as anticipated by theory [16]). Relatively large thermal fluctuations are needed to create lower-free-energy droplet phases from stripes. These large fluctuations are related to the same processes as govern the mobility of the domains. They are also influenced by impurities.
(3) Since boundary energies depend on temperature and the characteristic size of domain features depends exponentially on temperature, changing temperature allows the characteristic size of domain patterns to be manipulated easily.
(4) We find a close connection between surface morphology and domain structure: domain formation can be used to manipulate step structure and step structure can be used to influence domain structure.

Acknowledgments

The authors thank Peter Feibelman, François Leonard, and Brian Swartzentruber for many helpful discussions. This work was supported by the Department of Energy, Office of Basic Energy Sciences, Division of Materials Sciences. Sandia is a multiprogram laboratory operated by Sandia Corporation, a Lockheed Martin company, for the United States Department of Energy under Contract no DE-AC04-94AL85000.

References

[1] Garel T and Doniach S 1982 *Phys. Rev.* B **26** 325
[2] Seul M and Wolfe R 1992 *Phys. Rev.* A **46** 7519
[3] Langer S A, Goldstein R E and Jackson D P 1992 *Phys. Rev.* A **46** 4894
[4] Kashuba A B and Pokrovsky V L 1993 *Phys. Rev.* B **48** 10 335
[5] Dickstein A J *et al* 1993 *Science* **261** 1012
[6] Seul M and Andelman D 1995 *Science* **267** 476
[7] Keller D J, McConnell H M and Moy V T 1986 *J. Phys. Chem.* **90** 2311
[8] Andelman D, Brochard F and Joanny J-F 1987 *J. Chem. Phys.* **86** 3673
[9] McConnell H M 1991 *Annu. Rev. Phys. Chem.* **42** 171
[10] Keller S L and McConnell H M 1999 *Phys. Rev. Lett.* **82** 1602
[11] Marchenko V I 1981 *JETP Lett.* **33** 381
[12] Alerhand O L, Vanderbilt D, Meade R D and Joannopoulos J D 1988 *Phys. Rev. Lett.* **61** 1973
[13] Hurley M M and Singer S J 1992 *Phys. Rev.* B **46** 5783
[14] Vanderbilt D 1992 *Surf. Sci. Lett.* **268** L300
[15] Sagui C and Desai R C 1994 *Phys. Rev.* E **49** 2225
[16] Ng K-O and Vanderbilt D 1995 *Phys. Rev.* B **52** 2177
[17] Sagui C and Desai R C 1995 *Phys. Rev.* E **52** 2807
[18] Lu W and Suo Z 2001 *J. Mech. Phys. Solids* **49** 1937
[19] Kern K *et al* 1988 *Phys. Rev. Lett.* **67** 855
[20] Zeppenfeld P *et al* 1995 *Surf. Sci.* **342** L1131
[21] Zandvliet H J W *et al* 1998 *Phys. Rev.* B **57** R6803
[22] Pohl K *et al* 1999 *Nature* **397** 238
[23] Ellmer H *et al* 2001 *Surf. Sci.* **476** 95
[24] Thayer G E *et al* 2001 *Phys. Rev. Lett.* **86** 660
[25] Plass R *et al* 2001 *Nature* **412** 875
[26] Bauer E 1994 *Rep. Prog. Phys.* **57** 895
[27] Tromp R M and Reuter M C 1991 *Ultramicroscopy* **36** 99
[28] Plass R and Kellogg G L 2000 *Surf. Sci.* **470** 106
Kellogg G L and Plass R 2000 *Surf. Sci.* **465** L777
[29] Henrion J and Rhead G E 1972 *Surf. Sci.* **29** 20
[30] Camarero J *et al* 1998 *Phys. Rev. Lett.* **81** 850
[31] Müller S *et al* 2001 *J. Phys.: Condens. Matter* **13** 1793
[32] Meyer G, Michailov M and Henzler M 1988 *Surf. Sci.* **202** 125

[33] Müller B H, Schmidt Th and Henzler M 1997 *Surf. Sci.* **376** 123
[34] Nagl C *et al* 1994 *Surf. Sci.* **321** 237
[35] Braun J and Toennies J P 1996 *Surf. Sci.* **368** 226
[36] Chu Y S, Robinson I K and Gewirth A A 1997 *Phys. Rev.* B **55** 7945
[37] Stoycheva A D and Singer S J 2000 *Phys. Rev. Lett.* **84** 4657
[38] Fisher M E and Ferdinand A E 1967 *Phys. Rev. Lett.* **19** 169
[39] Schmid A K, Hwang R Q and Bartelt N C 2000 *Science* **290** 1561
[40] Pai W W, Swan A K, Zhang Z Y and Wendelken J F 1997 *Phys. Rev. Lett.* **79** 3210
[41] Hannon J B, Heringdorf F J M Z, Tersoff J and Tromp R M 2001 *Phys. Rev. Lett.* **86** 4871 and references therein
[42] Ozcomert J S, Pai W W, Bartelt N C and Reutt-Robey J E 1993 *Surf. Sci.* **293** 183
[43] Marchenko V I 1980 *Zh. Eksp. Teor. Fiz.* **52** 129
[44] Rickman J M and Srolovitz D J 1993 *Surf. Sci.* **284** 211
[45] Phaneuf R J, Bartelt N C, Williams E D, Swiech W and Bauer E 1991 *Phys. Rev. Lett.* **67** 2986
[46] Alerhand O L, Berker A N, Joannopoulos J D, Vanderbilt D, Hamers R J and Demuth J E 1990 *Phys. Rev. Lett.* **64** 2406
[47] Williams E D and Bartelt N C 1991 *Science* **251** 393
[48] Campbell C T and Koel B E 1987 *Surf. Sci.* **183** 100
[49] Feibelman P J 2000 *Phys. Rev. Lett.* **85** 606
[50] Pohl K *et al*, unpublished